Marine Geology 363 (2015) 191–201

Contents lists available at ScienceDirect

Marine Geology

journal homepage: www.elsevier.com/locate/margeo

Redistribution of multi-phase particulate organic carbon in a marine shelf and canyon system during an exceptional river flood: Effects of Typhoon Morakot on the Gaoping River–Canyon system

Robert B. Sparkes [a,b,*,1], In-Tian Lin [c], Niels Hovius [b,2], Albert Galy [b,3], James T. Liu [d], Xiaomei Xu [e], Rick Yang [d]

[a] Department of Materials Science and Metallurgy, University of Cambridge, Pembroke Street, Cambridge, UK
[b] Department of Earth Sciences, University of Cambridge, Downing Street, Cambridge, UK
[c] Department of Geosciences, National Taiwan University, Roosevelt Road, Taipei, Taiwan
[d] Department of Oceanography, National Sun Yat-sen University, Kaohsiung, Taiwan
[e] Earth System Science, University of California, Irvine, CA, United States

ARTICLE INFO

Article history:
Received 7 November 2014
Received in revised form 17 February 2015
Accepted 21 February 2015
Available online 25 February 2015

Keywords:
Taiwan
Typhoon Morakot
Turbidite
Carbon
Export
Burial

ABSTRACT

Volumetrically, turbidity currents are the prime suppliers of sediment to the deep sea, and conveyors of organic carbon from the terrestrial biosphere and submarine shelf into marine depositional basins. They result from complex processes of erosion, transport and deposition that can be difficult to study in detail. Here we present data from the Gaoping submarine canyon system, off SW Taiwan, which was perturbed in 2009 by the addition of flood deposits following Typhoon Morakot and sampled by gravity coring less than 2 months after the event. We use the different origins of organic carbon, distinguished by their carbon and nitrogen concentrations and $\delta^{13}C$ and $\delta^{15}N$ isotopic composition, to compare and contrast standard and extreme sedimentological conditions. Using well-constrained end-members, the results were de-convolved into inputs of metamorphic and sedimentary fossil organic carbon eroded within the Gaoping River basin, terrestrial non-fossil carbon and marine organic matter. In the upper Gaoping Canyon, sedimentation is dominated by the highly-localised hyperpycnal input of river washload and submarine sediment slumps, each associated with extensive flooding following Typhoon Morakot, whilst the shelf experienced deposition and reworking of hemi-pelagic marine sediments. A terrestrial signal is also found in the core-top of a fine-grained shelf sample over 20 km from the Gaoping Canyon, in a region normally dominated by marine carbon deposition, showing that Morakot was an unusually large flood event. Conversely, sediment from just above the canyon thalweg contains 0.23 wt.% depth-averaged marine organic carbon (37% of the TOC content) implying that terrestrial OC-dominated turbidites are tightly constrained within the canyon. Hyperpycnal processes can lead to the rapid and efficient transport of both terrestrial and submarine sediments to more permanent burial locations.

1. Introduction

Erosion and export of solid matter by small mountain rivers are responsible for a disproportionate amount of sediment transport and particulate organic carbon transfer globally (e.g. Milliman and Syvitski, 1992). When this material reaches the ocean it tends to be deposited in large submarine fans or canyon systems, or transported into the deep ocean or subduction trenches. Organic matter can be trapped within the resulting sediments and potentially preserved on geological timescales (Galy et al., 2007; Kennedy and Wagner, 2011). Understanding the contribution of various forms of organic carbon to this sedimentary burial flux can enhance insight into the role of coupled terrestrial erosion and marine deposition in the global carbon cycle. In addition, the intimate association of organic matter with clastic sediment may also give new constraints on the sourcing and routing of sediment in submarine fans and canyon systems.

The combination of fast tectonic uplift (5–7 mm yr^{-1}; Teng, 1990) and frequent typhoons leads to export of a large amount of terrestrial sediment to the ocean from Taiwan (Dadson et al., 2003). As the island is situated near to the biologically productive tropical belt, large amounts of organic carbon from various sources are transferred together with this sediment, including recently produced material ($OC_{biosphere}$ — following the classification of Kao et al. (2014)) from soils, standing biomass and modern woody debris harvested from

* Corresponding author at: School of Earth, Atmospheric and Environmental Sciences, University of Manchester, Oxford Road, Manchester M13 9PL, UK.
E-mail address: robert.sparkes@manchester.ac.uk (R.B. Sparkes).
[1] Now at University of Manchester, Oxford Road, Manchester, UK.
[2] Now at Helmholtz-Zentrum Potsdam, Deutsches GeoForschungsZentrum GFZ, Telegrafenberg, Germany.
[3] Now at CRPG-CNRS-Université de Lorraine BP20, 54501 Vandœuvre-lès-Nancy, France.

http://dx.doi.org/10.1016/j.margeo.2015.02.013

hillslopes and floodplains (West et al., 2011) and several types of ancient carbon (OC_{petro}), from lignite to graphite, eroded from exposed bedrock on the island (Dickens et al., 2004; Beyssac et al., 2007; Hilton et al., 2011). Work on Taiwanese rivers has shown that remobilisation of OC_{petro} from rock debris contained in landslide deposits within the fluvial channel network occurs throughout the year, but that large rainfall/flood events add $OC_{biosphere}$ to the suspended load (Hilton et al., 2008, 2012). Clastic sediment concentration in rivers draining the Taiwan mountains can increase by two orders of magnitude during storms, leading to an increase of fluid density and the formation of hyperpycnal plumes and turbidity currents where these rivers reach the ocean. Such density currents can quickly and efficiently transport sediments into marine basins (Dadson et al., 2005; Goldsmith et al., 2008; Masson et al., 2010; Liu et al., 2012). This, along with high submarine deposition rates for these conditions, can suppress marine remineralisation of organic matter and lead to the sequestration of terrestrial particulate organic carbon as well as marine carbon picked up in transit. Efficient (>70%) reburial of eroded fossil carbon has been observed in both hypopycnal and hyperpycnal systems off Taiwan (Kao et al., 2014), showing that terrestrial erosion and offshore transfer and burial can be a net export of carbon from the atmosphere, via the biosphere into the ocean. In contrast, deposition on a shallow marine shelf is likely to be only temporary, and organic carbon may be more prone to preservation on geological timescales if it can be transported further offshore, into a deeper basin. Organic carbon is prone to degradation in shelf sediments (Arndt et al., 2013), which will impact on the burial efficiency of the entire land–ocean sedimentary system, and therefore understanding the location and form of temporary deposits is important for quantifying POC from source to sink.

Whilst the mobilisation and fluvial transfer of particulate organic carbon to the coastline of rapidly eroding systems such as Taiwan have been observed and measured (Hilton et al., 2008, 2011), and the presence of terrestrially sourced carbon in deep marine deposits demonstrated (Weijers et al., 2009; Masson et al., 2010; Kao et al., 2014), less is known about the offshore transport of organic carbon linking source and sink. Studies of exhumed ancient turbidite systems allow for detailed lateral and vertical correlation (e.g. Amy and Talling, 2006), but the sediment and OC sourcing mechanisms and conditions are unknown. Here, we present a study of organic carbon contained in sediments of the Gaoping River in southwest Taiwan, and the marine shelf and canyon system into which it drains. These sediments were sampled within 2 months after passage of Typhoon Morakot in 2009 caused a flood with an estimated return time of 50–200 years (Chu et al., 2011) from a range of locations along the routing system. Opportunities to link identifiable extreme events and multiple offshore samples are extremely rare, and their content gives insight into the origin, marine transfer and offshore burial of particulate organic carbon (POC) during a large flood. Such events may be disproportionately important to burial fluxes over longer time scales. Additional samples collected earlier within the same system allow for some comparison with regular conditions.

2. Regional setting

The Gaoping River is the second largest in Taiwan, draining an area of 3257 km^2 with a mean annual discharge of 8.5×10^9 m^3 (Huh et al., 2009b), giving an annual runoff of 2.60 m, and an average erosion rate of 4.5 mm yr^{-1} (Dadson et al., 2003). It erodes mostly Miocene-age sedimentary rocks and older metasediments in the mountains of the Central Range, before crossing the recent sediments of the Pingtung plain and entering the South China Sea at Kaohsiung. Here, material can move into the Gaoping Canyon, a sinuous incision of the shelf and slope off SW Taiwan, until it reaches the Manila Trench, 260 km offshore. The canyon head is located about 1 km from the river mouth, in a marine shelf with a width of 45 km. At the shelf edge, the canyon floor is located 500 m below the adjacent shallow marine bathymetry, incised into young ocean sediments. This ensemble is set within an accretionary prism formed due to subduction of South China Sea ocean floor in the Manila Trench. Long-shore currents off the Kaohsiung coast are generally weak and of variable direction (Liang et al., 2003), potentially bringing muds from either flank into the canyon.

In a region of high sea surface temperatures and relatively low salinity, fluvial sediment concentrations in excess of 36 g l^{-1} can lead to hyperpycnal behaviour of river discharge plumes (Dadson et al., 2005; Oppo and Sun, 2005; Chiang and Yu, 2008). This threshold could be lower due to saline incursion at the river mouth and suspended sediment concentrations of 21.72 g l^{-1} are known to have led to density currents in the Gaoping Canyon (Liu et al., 2012). Hyperpycnal conditions are most likely to occur during river flooding and/or coastal storms (Mulder et al., 2003; Goldsmith et al., 2008). When depositing sediment, this type of flow might lead to a turbidite sequence (Liu et al., 2009). At lower sediment concentrations, a hypopycnal plume may build at the river mouth. This turbid plume can spread at the ocean surface, causing fall out of suspended sediment and deposition over a wide area, with the plume behaviour dependent on discharge, buoyancy and surface currents. This process can lead to deposition of river load on the shelf as well as in the canyon. The Gaoping River is hypopycnal during regular discharge conditions and is only likely to be hyperpycnal for some hours to days during typhoon floods (Liu et al., 2013). Alternatively, larger volumes of sediment, including terrestrially sourced material, can be remobilised by slumping in the margins of the submarine canyon, and turbidity currents could ensue (Mulder and Cochonat, 1996).

On 7–10th August 2009 the Gaoping catchment was subjected to a major (estimated return time 50–200 years; Chu et al., 2011) flood following Typhoon Morakot. Although only a category 3 typhoon, Morakot had a particularly strong impact due to its halt over southern Taiwan and connection with a low pressure trough extending east from the Bay of Bengal. This trough fed heat and water vapour into the typhoon, leading to three days of rainfall with a recorded maximum of 2777 mm precipitation (Ge et al., 2010). Landslides affected about 130 km^2 of the Gaoping River basin, 3.9% of the catchment area (West et al., 2011), releasing an estimated 285 million tonnes of sediment. As a result, suspended sediment concentrations in the Kaoping River reached extremely high levels (60 g l^{-1}; Liu et al., 2012). As a result, hyperpycnal flows initiated at the river mouth and flowed through the Gaoping Canyon into the Manila trench (Kao et al., 2010; Su et al., 2012). Breakage of communication cables indicates that a turbidity current on 9th August travelled more than 150 km along the canyon in water depths up to 3700 m. A second submarine density flow initiated three days later in either the Gaoping Canyon or nearby Fangliao Canyon and led to cable breaks up to 375 km along the Gaoping Canyon–Manila Trench system (Carter et al., 2014).

This study considers the organic carbon content and composition of eight cores collected up to 35 km offshore Kaohsiung soon after Typhoon Morakot, from the Gaoping shelf and slope, in water depths of up to 1200 m. These cores were collected by the ship Ocean Researcher 1, during cruise 915 between 28 Sept. and 4 Oct., 2009, using a variety of methods including box, gravity and piston coring. Whilst it is possible for submarine sediment flows to be erosive and/or leave no trace, the upper sections of these cores are assumed to represent post-Morakot sediments. Fig. 1 shows the location of the core sites. Core sites K1 and K12A were proximal to the Gaoping River (2.5 km and 10 km offshore respectively), in or near the canyon thalweg. Cores K25B, K8, K8X and K15 were collected in an offshore-transect along the Gaoping Canyon. Core K11A was collected from incised shelf material on the flank of the Gaoping Canyon, 150 m above the thalweg, Core L9 was collected from the shelf, 20 km southeast of the canyon. Typical shelf sedimentation in this area occurs at an annual deposition rate of about 0.6 g cm^{-2} yr^{-1} (Huh et al., 2009a). These materials are complemented by 29 cores from an offshore sampling campaign in 2001, during more normal sedimentary conditions. These cores were arranged in a fan shape with an internal grid pattern, providing regular samples of an

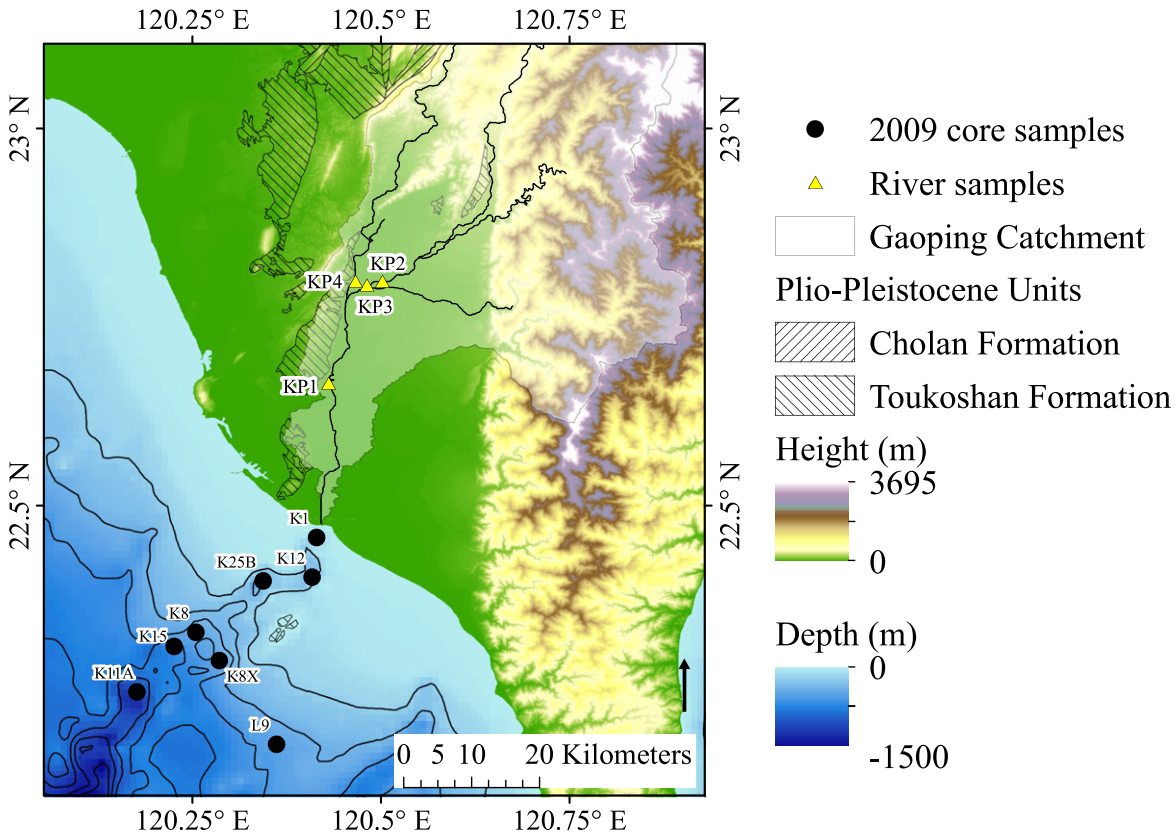

Fig. 1. Combined topographic and bathymetric map of the Gaoping River and Canyon, showing the tributaries of the Gaoping River, the location of terrestrial and offshore samples and the exposure of the Plio-Pleistocene Cholan and Tuokoshan formations.

area extending 35 km offshore and 9–14 km either side of the Gaoping Canyon and covering approximately the same area as the Morakot cores (see Fig. 2). In addition, terrestrial samples were collected in the floodplain of the Gaoping River in November 2009. Samples were collected from tributaries draining both the Central Range and the coastal plain, and from a range of locations including reworked fluvial sand bars, storm overbank deposits and channel bank deposits (see Fig. 1).

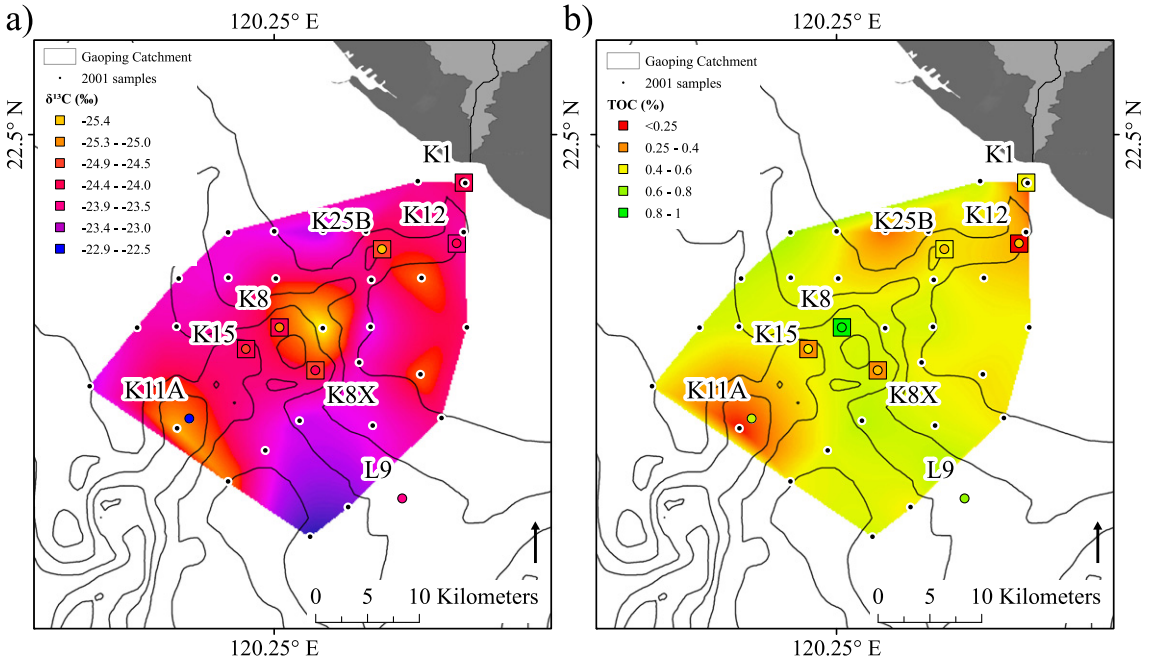

Fig. 2. Two maps comparing isotopic and elemental data from 2001 and 2009 samples. Post-Morakot cores are labelled, 2001 samples are shown as small black points. For the post-Morakot cores, squares represent sandy sections of cores and circles represent mud caps. In each case the core-top of sample L9 has been removed, as it has a significantly different isotopic and elemental composition (see Discussion). a) Core-top TOC from 2001 and core-average TOC from 2009. b) Core-top $\delta^{13}C$ from 2001 and core-average $\delta^{13}C$ from 2009. 200 m bathymetric contours are shown.

3. Materials and methods

Core samples from Typhoon Morakot were split, photographed and cut in 1 cm slices, which were then freeze-dried. 5 g aliquots of selected 1 cm horizons were collected; these horizons were chosen based on variations in grain-size, colour, or visible POC content. Samples were homogenised into a fine powder using a Retsch PM-400 agate ball-mill grinder, achieving a median diameter of 9.2 μm, as measured by a Malvern Instruments Mastersizer 2000 laser grain size analyzer. 0.5 g of sample was then de-carbonated using 1 N HCl for 180 min at 80 °C. Samples were weighed before and after de-carbonation in order to correct for the reduction in mass due to carbonate grain dissolution when calculating the concentration of organic carbon and nitrogen in the samples. De-carbonated powders were rinsed with de-ionised water and dried at 80 °C overnight before being re-homogenised and stored in a desiccator. 20 mg of material was placed in a tin capsule and analysed in a Delta V EA-IRMS. Measurements were taken of Total Organic Carbon (TOC), Total Organic Nitrogen (TON), stable carbon isotopes ($\delta^{13}C$) and stable nitrogen isotopes ($\delta^{15}N$), following the standard procedure at the Godwin Laboratory, University of Cambridge (Hilton et al., 2008, 2012; Smith et al., 2013). The long-term average relative difference was <0.075% for C and N, and long-term average standard deviation was 0.05% for $\delta^{13}C$ and 0.3% for $\delta^{15}N$. Cores from the 2001 campaign have been analysed for TOC content and $\delta^{13}C$ values on a Delta XP IRMS following Hung et al. (2012). Radiocarbon measurements of individual aliquots were made at the KCCAMS facility at University of California, Irvine, by a compact accelerator mass spectrometer (NEC 0.5MV 1.5SDH-2 AMS system, from National Electrostatics Corporation, with a modified NEC MC-SNIC ion-source (Southon and Santos, 2007)) on graphite prepared from samples. The relative percent error of day-to-day analysis, including extraction, graphitization and AMS measurement, is between 2.5 and 3.0‰ based on secondary standards measured in the past, which is equivalent to ≤35 yrs of error for 10,000-year-old samples (Xu et al., 2007).

4. Results

Visual inspection of canyon cores found coarse and medium sand lower in the cores, which fined upward into a mud cap. It was assumed that these sediments were deposited following Typhoon Morakot and that, where more than one sand–mud sequence was present, the uppermost couplet represented the Morakot event. This sequence was 37 cm thick in core K1 but thinned quickly offshore to a few cm. Woody clasts were sometimes seen within the sandy parts of the cores, up to 40 mm in length in K1. Offshore, cores K25B, K8, K8X and K15 contained finer grained material. Fine sandy layers at the base of the cores, thinning offshore and containing fibrous woody clasts, were covered by mud caps up to 5 cm thick, which contained microscopic POC. The canyon side and shelf cores, K11A and L9, contained clay-rich mud with mm-scale lamination. No macroscopic POC clasts were visible in these two cores, but microscopic analysis showed that both graphite and aged woody material were present. Annual deposition rate measurements (Huh et al., 2009a) suggest that only the shelf core tops represent Morakot-sourced material.

The core samples produced a range of geochemical values. TOC ranged from 0.21 to 0.36 wt.%, TON from 0.05 to 0.12 wt.%, leading to a C/N from 3.48 to 14.2, $\delta^{13}C$ from −26.0 to −22.5‰ and $\delta^{15}N$ from 1.29 to 3.30‰. Fig. 3a shows the range of data collected from each core in $\delta^{13}C$ vs. N/C space. Measured $\delta^{13}C$ values were highest in the slope cores and lowest in the woody-debris rich, sandy parts of canyon cores. Further descriptions of the core samples can be found in the supplementary information. Grain size, TOC and $\delta^{13}C$ profiles can be found in Fig. S1.

Sediment samples from the Gaoping River had low to moderate TOC values (0.16–0.37% with an average of 0.25%), $\delta^{13}C$ values ranging from −24.69 to −23.13‰ (Fig. 3d) and N/C values from 0.19 to 0.27. Woody debris collected from a flood deposit on the riverbank at site KP1 had very low $\delta^{13}C$ and N/C values, −26.5 to −27.0‰ and 0.011 to 0.015, respectively.

The 29 core-top samples from 2001 had TOC values ranging from 0.22 to 0.78% and $\delta^{13}C$ values ranging from −22.55 to −24.7‰ (Fig. 2). TOC values were low on the shallow shelf and in the deep canyon, with a higher TOC concentration away from the canyon. In general the shelf material had a higher $\delta^{13}C$ than the canyon. Low $\delta^{13}C$ values were found in the canyon, with higher $\delta^{13}C$ on the slope. The highest $\delta^{13}C$ values were found on the offshore part of the shelf, furthest from the Gaoping River mouth, whilst lowest $\delta^{13}C$ values were midway down the Gaoping Canyon at around 600 m water depth.

$\Delta^{14}C$ values in samples from cores K1, K11A and L9 ranged from −794 to −544‰ (Fig. 4a). This corresponds to a proportion of non-petrological organic carbon of 0.207 to 0.459 fraction modern (F_{mod}). $\Delta^{14}C$ and fraction modern (F_{mod}) are as defined by Stuiver and Polach (1977). The samples with the lowest F_{mod} were from the muddy section of core K1 nearest the head of the canyon, and the highest F_{mod} values were from shelf core L9.

4.1. Deconvolving organic carbon inputs to the Gaoping Canyon

Organic carbon in marine basins with a terrestrial feed can have several sources, principally standing biomass and soil-bound carbon ($OC_{biosphere}$), erosion of geologically young sediments and older rocks (OC_{petro}), and marine primary production (OC_{marine}), all of which have been reported in the Gaoping Canyon (Kao et al., 2014). The complex mixture of these sources, and their relative input cannot be quantified by a single measurement. A model was created to unmix a number of organic carbon sources, defined as a series of endmembers with distinct compositions. Sources, endmembers, and the method for unmixing them, follow below.

Modern biomass ($OC_{biosphere}$) can be mobilised from hillslopes into rivers by landsliding or surface run-off (Smith et al., 2013), and can exist as a wide range of particle sizes, from monomolecular films on particle surfaces and μm-scale soil components up to decameter tree trunks (West et al., 2011). Channel processes can cause shredding of the ends and sides of trunks, branches and bark, leading to flakes of woody material being carried along with the sediment load of the river, which were seen for example in core K8. Fresh terrestrial biomass eroded from Taiwan has isotopic values similar to local C3 biomass (Kao et al., 2014; Hilton et al., 2013). Analysis of fresh plant material from floodplain deposits sampled after Morakot gave $\delta^{13}C = -26.84$‰, $\delta^{15}N = -3$‰ and N/C = 0.013 (Source 1).

OC_{petro} is sourced by erosion of organic carbon-bearing rocks. Fossil carbon in rivers can have a range of compositions, depending on the geology from which it is extracted (Hilton et al., 2010). Within the Gaoping catchment area this falls into two broad categories, metamorphic carbon from the Central Range (Beyssac et al., 2007), in the form of semi- or fully-graphitized material (Beyssac et al., 2002), denoted as $OC_{petro\text{-}meta}$, and amorphous, lignite-grade carbon sourced from lower-grade Plio-Pleistocene foreland basin rocks (Chen et al., 2001; Sparkes et al., 2013), here classified as $OC_{petro\text{-}sed}$. Samples of lignite from the Cholan and Tuokoshan formations produced average values of $\delta^{13}C = -27.1$‰, $\delta^{15}N = 3.6$‰ and N/C = 0.011 (Source 2).

No direct measurements of metamorphic carbon-bearing units ($OC_{petro\text{-}meta}$) were made, instead suitable river and marine samples were used to take advantage of the integrating effects of erosion on heterogeneous systems. Metamorphic carbon-bearing formations have high $\delta^{13}C$ and N/C values (Hilton et al., 2010). Samples with geochemical properties least like $OC_{biosphere}$ were measured in both the river (KP2B) and offshore (K12–17 and K12–18). These were coarse-grained sandy samples in which no $OC_{biosphere}$ was observable by eye or with a microscope. These three samples had values of $\delta^{13}C = -23.1$ to −23.6‰, $\delta^{15}N = 1.64$ to 2.45‰ and N/C = 0.27 to 0.29 (Source 3).

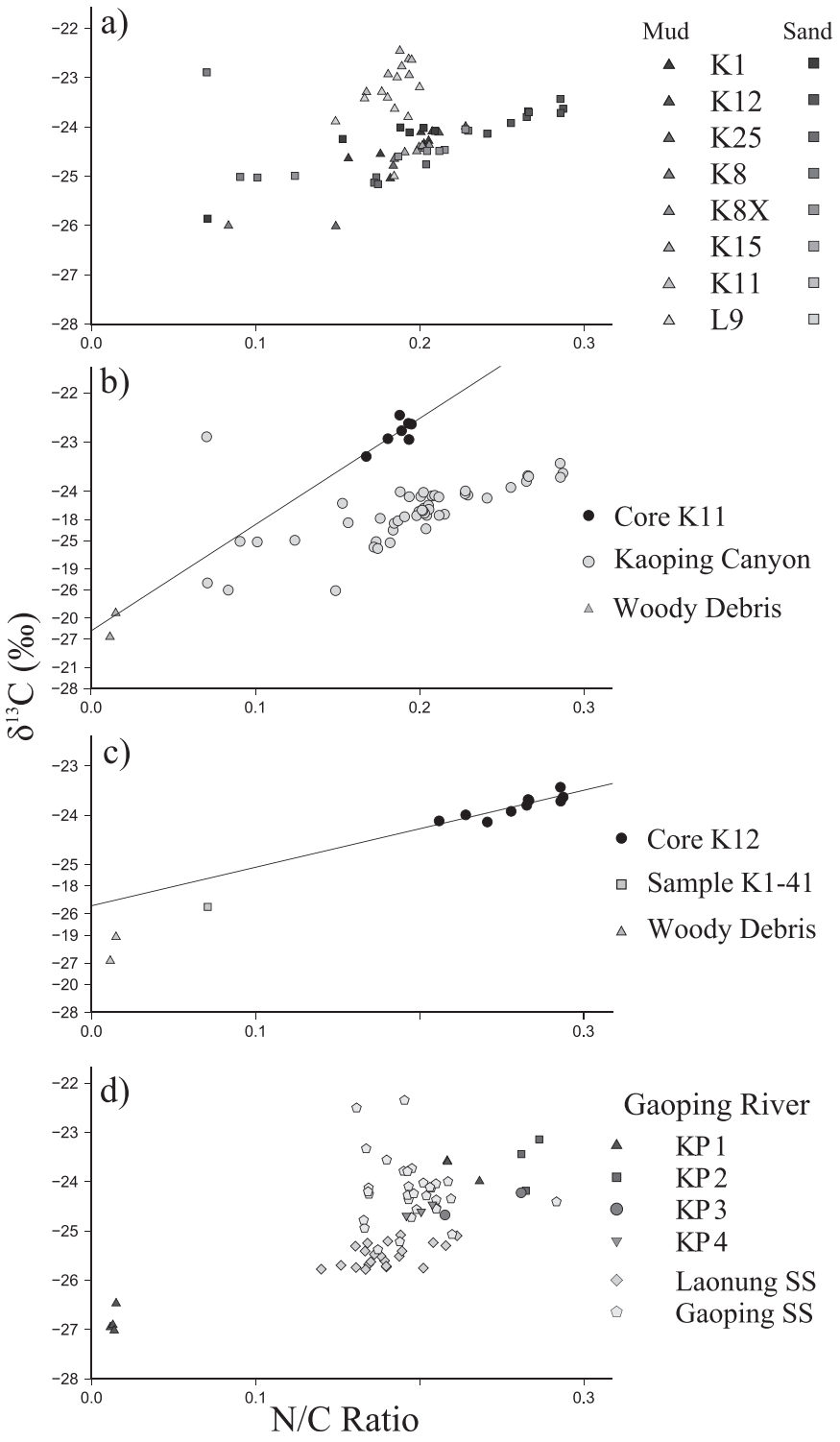

Fig. 3. Plots of $\delta^{13}C$ vs N/C ratio for terrestrial and offshore samples from 2009. a) All eight offshore cores, split into sandy (square markers) and muddy (triangular markers) sections of the cores. b) Core K11, the most distal of the cores in this study, plotted alongside the other canyon cores. This core has a significantly different isotopic composition to the others, although a linear regression line shows that it is still related to woody debris input. c) Core K12 plotted in $\delta^{13}C$–N/C space with K1–41 and Gaoping River CWD also plotted to highlight terrestrial biomass inputs. Variations in core K12 are also likely due to terrestrial biomass input. d) Samples from the Gaoping River, which plot in a similar location to the canyon cores.

OC_{marine} is usually very labile and re-mineralised easily within the water column and on the seafloor, giving rise to global preservation ratios on the order of 0.5% of OC_{marine} production (Hedges and Keil, 1995). However, high production rates of OC_{marine} compared to terrestrial input mean that OC_{marine} can be an important component of offshore sediments, with global OC_{marine} burial approximately equal to terrestrially-sourced OC (Hedges and Keil, 1995). Marine organic matter is relatively less depleted in nitrogen and ^{13}C than terrestrial vegetation. High-energy submarine transport mechanisms, such as turbidity currents, have the ability to re-suspend OC_{marine} from the seabed. This leads to reworking of previously deposited sediment, and replenishment of turbidity currents, driving auto-suspension and increasing

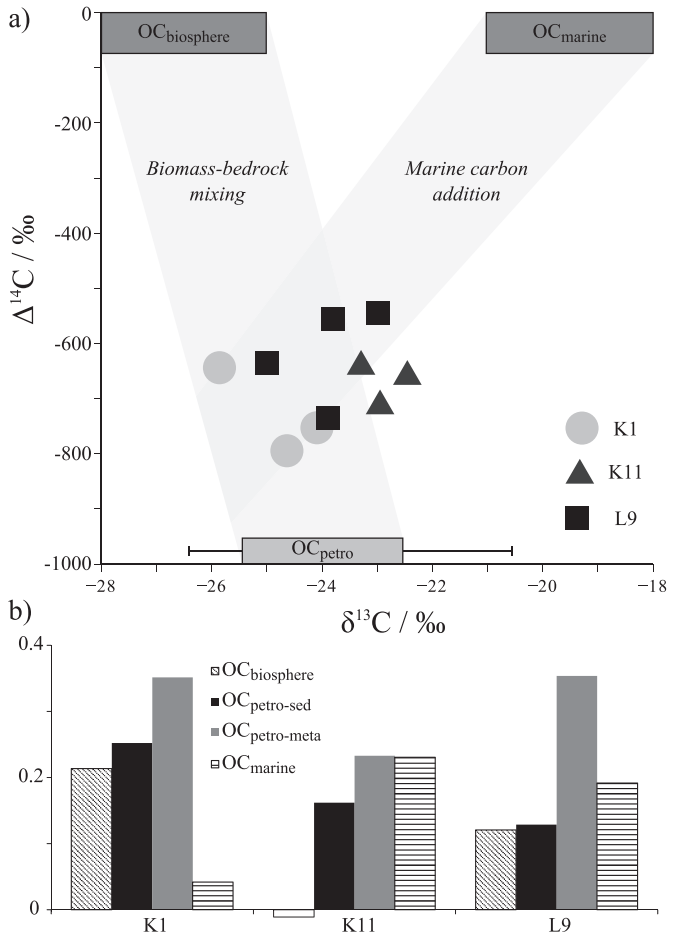

Fig. 4. A comparison of radiocarbon and stable carbon isotopic compositions for ten samples from cores K1, K11A and L9. Also shown are typical compositions of C3 plants, soils, marine carbon and bedrock carbon (Hilton et al., 2010; Kao et al., 2003).

run-out distances (Bagnold, 1962). This is one of the mechanisms by which remobilised OC_{marine} can be transported from the shelf to the deep ocean (Source 4).

The mixture of sources present in each sample was determined. This was achieved by defining a series of endmembers that enveloped the distribution of values seen in the sample set, and applying a series of simultaneous equations that un-mixed each sample to calculate the input of each endmember to the mixture. Coupled carbon and nitrogen measurements gave four readings for each sample: TOC, TON, $\delta^{13}C$ and $\delta^{15}N$, which allow for a maximum of four identifiable end-members. Defining suitable endmembers sometimes necessitated combining two carbon sources into a single endmember, or using two endmembers to fully characterise one source.

$OC_{biosphere}$ (Source 1) and $OC_{petro\text{-}sed}$ from the sedimentary Plio-Pleistocene formations (Source 2) had very similar $\delta^{13}C$ and N/C values. Despite differences in $\delta^{15}N$ values (−3 c.f. 3.6‰), in the absence of $\Delta^{14}C$ measurements for all samples it was necessary to combine these two sources into one endmember. Endmember 1 was defined with values of N/C = 0.015, $\delta^{13}C = -27$‰, $\delta^{15}N = 1$‰. When radiocarbon measurements were available, these two sources could be separated.

$OC_{petro\text{-}meta}$ (Source 3) required two endmembers to account for the range of geochemical values measured. These endmembers were based on the samples least like Sources 1 and 2, and the measurements of Hilton et al. (2010). Endmember 2 was defined as having N/C = 0.285, $\delta^{13}C = -23.1$‰, $\delta^{15}N = 3$‰, whilst Endmember 3 has N/C = 0.282, $\delta^{13}C = -23.63$‰, $\delta^{15}N = 1$‰.

OC_{marine} (Source 4) was investigated by Kao et al. (2003), who measured ocean sediments from offshore northern Taiwan. Endmember 4 was defined using their results from the mid and outer shelf area, with N/C at the Redfield ratio, 0.056, $\delta^{13}C = -20$‰, $\delta^{15}N = 4.5$‰.

Endmember compositions used in the unmixing model are listed in Table 1. The four end-members were differentiated using simultaneous mixing equations:

$$TOC_{sample} = \sum f_i \times TOC_i$$

$$TON_{sample} = \sum f_i \times TON_i$$

$$\delta^{13}C_{sample} \times TOC_{sample} = \sum f_i \times \delta^{13}C_i \times TOC_i$$

$$\delta^{15}N_{sample} \times TON_{sample} = \sum f_i \times \delta^{15}N_i \times TON_i$$

$$\sum f_i = 1.$$

Multiplying f_i, the fraction of each component in the sample, by TOC_i, the carbon content of that sample, gave the carbon contribution of each end-member to the sample. The uncertainty associated with each result was approximately 0.05 wt.% carbon, and a component with an estimated contribution less than this may not have been present at all. When radiocarbon analyses were also available, for a subset of samples from cores K1, K11A and L9, a mass-balance equation was used to distinguish $OC_{biosphere}$ from $OC_{petro\text{-}sed}$:

$$\Delta^{14}C_{sample} \times TOC_{sample} = \sum f_i \times \Delta^{14}C_i \times TOC_i.$$

In this case, the OC_{petro} endmembers had radiocarbon values of $\Delta^{14}C = -1000$‰, whilst $OC_{biosphere}$ had $\Delta^{14}C = 0$‰ and OC_{marine} had $\Delta^{14}C = -59$‰ following the study of Kao et al. (2014).

4.2. Results of endmember-unmixing calculations

Core-specific results of the unmixing calculations are contained in the supplementary information, Table S1 and Fig. S1. Core-averaged inputs of OC are shown in Fig. 5. Canyon cores (K1, K12, K25, K8X, K15) contained little to no OC_{marine} (0.00 ± 0.03 wt.% C), with only the sandy, OC-rich base of core K1 reporting any significant OC_{marine} content (Fig. 6). Overall $OC_{petro\text{-}meta}$ was the most abundant endmember in the canyon cores, with little variation between cores or with depth downcore (overall average of K1, K12A, K25B, K8X and K15 = 0.27 ± 0.07 wt.% C), whilst Endmember 1 contributed approximately half as much OC (average = 0.15 ± 0.16 wt.% C). This bimodal input can also be seen in plots of $\delta^{13}C$ vs. N/C (Fig. 3a and c). Thus, the samples show a linear mixing trend between typical terrestrial biomass and petrogenic carbon values without deflection towards marine carbon compositions. There is a strong correlation between Endmember 1 and TOC ($R^2 = 0.88$, $p < 0.0001$) that is much weaker for $OC_{petro\text{-}meta}$ and OC_{marine} ($R^2 = 0.13$ and 0.28, $p = 0.02$ and 0.0003 respectively) suggesting that influx of $OC_{biosphere}$ and/or $OC_{petro\text{-}sed}$ is mostly responsible for fluctuations in TOC. Fig. 6 shows this pattern throughout core K1. $\Delta^{14}C$ measurements from this core suggest that the $OC_{biosphere}$ and $OC_{petro\text{-}sed}$ contributed roughly equivalent amounts to carbon deposition at this site (Fig. 4b).

According to calculations, OC_{marine} was present (0.20 ± 0.08 wt.% C) in samples K11A and L9, both located on the shelf. $OC_{petro\text{-}meta}$

Table 1
End-members for 4-component mixing where ^{14}C measurements are unavailable.

End-member	[C] (wt.%)	[N] (wt.%)	$\delta^{13}C$ (‰)	$\delta^{15}N$ (‰)
1 − $OC_{petro\text{-}meta1}$	0.466	0.133	−23.1	3
2 − $OC_{petro\text{-}meta2}$	0.117	0.033	−23.63	1
3 − $OC_{biosphere}$ + $OC_{petro\text{-}sed}$	60	0.9	−27	1
4 − OC_{marine}	40	6.68	−20	4.5

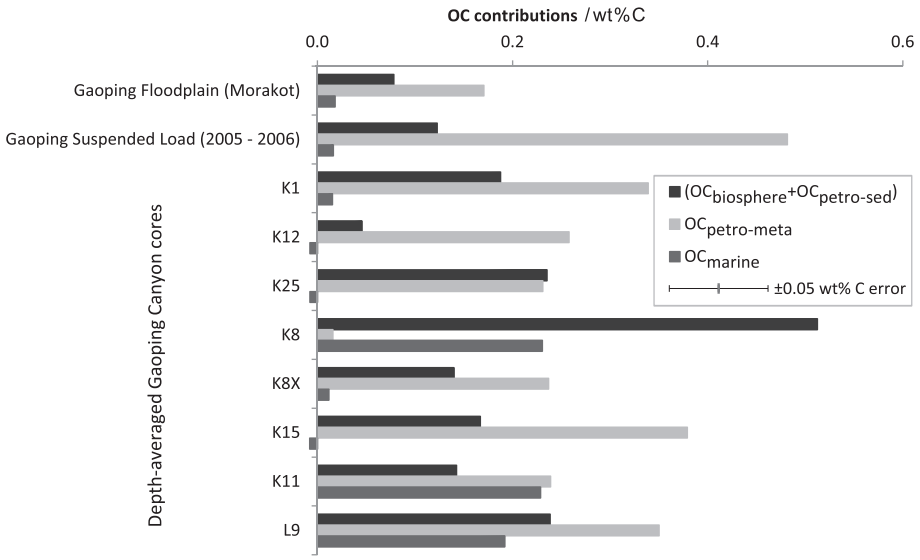

Fig. 5. Depth-averaged results of endmember unmixing for each core. Black bars represent the contribution of terrestrial biomass (both modern plant material and recycled low-grade sedimentary carbon), light grey bars represent bedrock fossil carbon and mid-grey bars represent marine biomass. Cores are arranged in a proximal to distal order. Suspended sediment samples from the Gaoping River are also shown. These were collected prior to Morakot (Hilton et al., 2010) and represent an alternative sedimentary routing mechanism dominated by soil erosion and suspended load transport rather than routing of woody debris. Error bars corresponding to estimated uncertainty of ± 0.05 wt.% C in the unmixing calculation are shown in the legend; negative reported values are within this uncertainty.

content in these cores was similar to the canyon cores (0.30 ± 0.08 wt.% C), as was Endmember 1 (0.19 ± 0.07 wt.% C). Incorporating radiocarbon results showed that K11A contained little-to-no $OC_{biosphere}$, but that core L9 contained equal amounts of $OC_{biosphere}$ and $OC_{petro\text{-}sed}$ (Fig. 4b).

Plotting $\delta^{13}C$ against $\Delta^{14}C$ for terrestrial Taiwanese samples reveals a mixing zone between OC_{petro} and $OC_{biosphere}$ (Kao et al., 2014). When our results are plotted in this space (Fig. 4a) core K1 and the core top of L9 sit within this mixing zone whilst the slope cores (K11A and L9) deviate from this trend towards the marine carbon composition. Simple addition of marine organic matter would lead to a trend directly from the plant–bedrock mixing line towards the marine carbon composition. Core L9 measurements plot accordingly, whereas the data from core K11A does not (Fig. 4a). It has a diminished plant biomass contribution

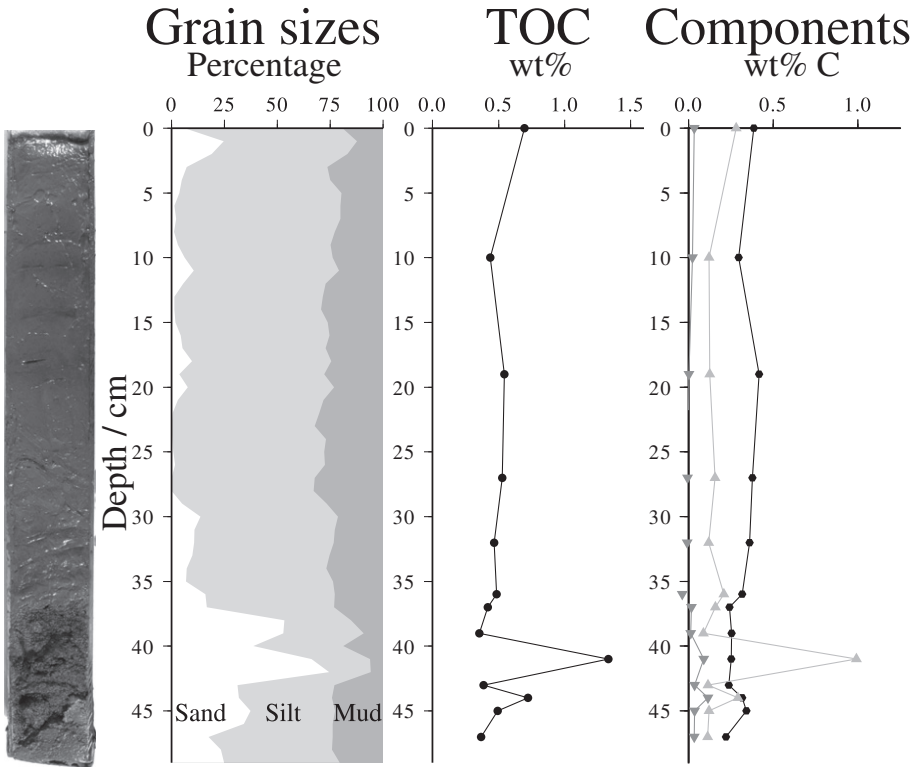

Fig. 6. Grain-size, TOC and end-member profiles through core K1. In the component plots, black circles are fossil, mid-grey upwards triangles are terrestrial biomass, light grey inverted triangles are marine biomass. Variations in TOC appear to be most strongly related to the amount of terrestrial biomass.

and an increased marine carbon input, as was seen in the endmember unmixing calculations.

Gaoping River sediment was dominated by $OC_{petro\text{-}meta}$ (0.17 ± 0.06 wt.% C c.f. 0.08 ± 0.03 wt.% C from Endmember 1), with OC_{marine} below the uncertainty (0.05%) of the unmixing method (0.02 ± 0.03 wt.% C on average) as expected from a purely continental sediment. Using the end-member defined in this study, suspended sediment collected from the Laonung and Gaoping Rivers prior to Typhoon Morakot (Hilton et al., 2010) would return more OC_{marine} in these calculations and the difference with the post-Morakot bedload samples is likely to reflect changes in the terrestrial end-members induced by the extreme event.

5. Discussion

5.1. Comparing Morakot with standard conditions

Prior to Typhoon Morakot, Hilton et al. (2010) collected fluvial suspended sediment samples from the Gaoping and Laonung Rivers. In Fig. 3d, the $\delta^{13}C$ and N/C values measured on these samples are compared with equivalent post-storm data. N/C was slightly lower and $\delta^{13}C$ higher before the storm. One explanation for this could be an increased proportional contribution of C4 plant material before the storm. $\delta^{15}N$ values of fluvial sediment pre- and post-Morakot differed substantially. Pre-Morakot sediments had $\delta^{15}N$ values of 3.38 ± 0.91‰ (Hilton et al., 2010), higher than the post-Morakot values of 1.40 ± 0.68‰, suggesting that there was a change in sediment sourcing during Morakot. Given that Taiwanese soils have ~4‰ higher $\delta^{15}N$ than their corresponding plants (Hilton et al., 2013), lower $\delta^{15}N$ values in post-Morakot fluvial samples indicate that whilst prior to the typhoon the river conveyed soil-rich material, sediments mobile during Morakot were enriched in biomass and woody debris, as suggested by West et al. (2011). Pre-Morakot suspended sediment samples (Hilton et al., 2010) are, therefore, not representative of the material delivered by the typhoon flood, and it is likely that sediment supplied to the offshore sediment dispersal system during the storm was different to that during more normal meteorological conditions (e.g. the 2001 samples). Gaoping suspended load sediments are similar to the 2001 offshore cores. Suspended river sediments have TOC = 0.69 ± 0.53 wt.% C, $\delta^{13}C = -24.2 \pm 0.6$‰; core tops from 2001 have TOC = 0.61 ± 0.12 wt.% C, $\delta^{13}C = -23.7 \pm 0.4$‰.

The post-Morakot cores show that lateral variations in carbon content and $\delta^{13}C$ can be sizeable and manifest over short distances. Their characteristics can be compared to the 2001 samples, to see whether the distribution of carbon following an extreme event is different to the patterns we assume to be more general. Since TN and $\delta^{15}N$ data are not available for samples collected in 2001, the comparisons are limited to TOC and $\delta^{13}C$ values only. Endmember mixing calculations are not possible with just these two measurements, but the distribution of OC and its isotopic value can still be used to perform a first-order comparison between cores collected in 2001 and post-Morakot.

On the submarine shelf about 20 km away from the canyon, core L9, interpreted to be rich in marine organic matter, matches well with the nearby high $\delta^{13}C$ samples from 2001. However, without the corresponding nitrogen measurements it is impossible to confirm the marine enrichment of these older samples using end-member-unmixing. L9 potentially represents approximately 1800 years of deposition at 0.24 mm yr^{-1} (Huh et al., 2009a), although reworking events may have removed or replaced some material during this time and deposition rates may have changed. The majority of the core is chemically homogenous, with a very constant isotopic ratio throughout and mm-scale laminations visible in photographs. The core-top however has a very different appearance, much darker in colour, and with geochemical properties similar to sediments retrieved from the upper canyon (see Fig. 3a). There is no evidence of these darker layers lower in the core, which means that either they have been eroded or destroyed by diagenesis, or this is a deposit unique to Morakot. This typhoon caused an unusually significant amount of flooding and fluvial discharge, which may have created a hypopycnal plume, during or after the main hyperpycnal flow, extending several tens of km across the Gaoping shelf and delivering terrestrially derived fine suspended sediment to locations, which are normally dominated by marine deposition.

Core K11A on the canyon flank did not match the nearby 2001 sample in TOC nor $\delta^{13}C$. Whilst the 2001 sample had low TOC, similar to the canyon samples, and a very light $\delta^{13}C$ composition suggesting dominance of terrestrial woody debris, organic carbon in core K11A was much more like the shelf material retrieved from core L9, with evidence of marine carbon admixture. Hence, the canyon thalweg domain is sharply defined, and shelf-style deposits can be found close to the canyon floor. This may be due to deep incision of the canyon into ancient shelf deposits, or to persistence of shelf-style deposition on the flanks of the canyon, above the level affected by gravity currents in the canyon thalweg. Excluding the core-top of L9, these two cores contain 32 ± 9% OC_{marine} as a percentage of Total Organic Carbon, showing that terrestrial carbon is preserved in Gaoping shelf sediments alongside OC_{marine}. The terrestrial OC is likely sourced from persistent hypopycnal delivery of river sediments and possible reworking during storms.

In comparison to the shelf sediments, more depleted $\delta^{13}C$ values were found in the Gaoping Canyon in both the 2001 and 2009 samples (Fig. 2), suggesting a greater contribution of carbon from terrestrial sources. Sediments collected within the Gaoping Canyon after Typhoon Morakot had an $OC_{petro\text{-}meta}$ content, depth-averaged across the entire core lengths, of 0.29 wt.% C and a depth-averaged $OC_{biosphere} + OC_{petro\text{-}sed}$ concentration of 0.15 wt.% C (Fig. 5). This composition contrasts with that of Gaoping River bedload samples, which were collected from overbank deposits and partially reworked fluvial sand bars two months after the storm. Whilst the $OC_{petro\text{-}meta}$ content was similar between these settings, 0.17 ± 0.06 wt.% C, the $OC_{biosphere} + OC_{petro\text{-}sed}$ component of the river bedload sediments, 0.08 ± 0.03 wt.% C, was only half that of the cores. The organic matter content of these cores is closer to that of river suspended load. The average amount of POC in the Gaoping River suspended load classed as $OC_{petro\text{-}meta}$ was 0.48 ± 0.20 wt.% C, whilst $OC_{biosphere} + OC_{petro\text{-}sed}$ was 0.12 ± 0.09 wt.% C, based on data from Hilton et al. (2010) analysed using the endmember unmixing procedure. Hilton et al. (2008) showed that in Taiwan suspended sediment and $OC_{biosphere}$ are disproportionally transported during extreme events. Thus the canyon samples contain much more terrestrial biomass than the river bedload, but similar to the average river suspended load and the flood-event suspended load, both as proportion per gramme of sediment and proportion of TOC. The source of the terrestrial material in offshore sediments is, therefore, likely to be suspended sediment rather than bedload material transported during the storm.

Core K8, containing large, fibrous, wood particles, had higher TOC concentrations than any of the 2001 samples. This concentration of carbon seems unique amongst the Morakot cores, and is likely due to density-size segregation during suspended load settling and bedload transport. Fibrous vegetation particles found in this core could result from shredding of tree bark and trunks during the particularly energetic fluvial transport conditions associated with Typhoon Morakot. Extreme variations in $\delta^{13}C$ seen in this core (as high as −22.9‰, with associated N/C values of 0.0704) may reflect variable proportions of C3 and C4 plant material down the core. Given the relatively small volumes of processed material, measured values are prone to effects of the presence of non-representative wood particles in individual samples.

5.2. Marine organic material incorporation during Morakot type turbidity current

During extreme storms, such as Morakot, the large volume of terrestrial sediment output can be complemented with shelf and canyon sediments reworked by several possible mechanisms. Particularly large typhoons can lead to abnormal sedimentary conditions on the shelf as

well as on land, with storm wave impact reactivating sediment from large areas of the continental shelf and delivering it to the submarine canyon and abyssal plain. Scouring of hemi-pelagic marine sediment from the canyon floor by the turbidity currents can add marine carbon to the submarine flows. Canyon margin slumps can combine recently deposited terrestrial sediment with slowly accumulated marine carbon. Transport of carbon-rich marine muds from shelf to slope and deep marine sedimentary systems throughout a typhoon has the potential to deliver a considerable amount of carbon to the deep ocean. Submarine landslides in the canyon flanks (Ramsey et al., 2006), during or after passage of turbidity currents can cut into the shelf stratigraphy and introduce material of varying age to the canyon floor. These processes have two potential effects on carbon burial and preservation. Remobilisation of previously deposited carbon can expose it to oxygenating conditions and the possibility of degradation, whilst the subsequent burial of this material within the large sedimentary deposits produced by turbidity currents can enhance the preservation potential compared to shallow burial on the shelf. The shelf cores had concentrations of $OC_{petro\text{-}meta}$ and Endmember 1 ($OC_{biosphere} + OC_{petro\text{-}sed}$) equivalent to the canyon cores, suggesting conservative addition of marine carbon to the terrestrial load, rather than a remineralisation and replacement of terrestrial OC on the shelf. Mountainous ocean islands experiencing extreme weather events can deliver large volumes of sediment (Carter et al., 2014) and organic carbon (Kao et al., 2014) to the ocean, which can lead to long-term sequestration of organic carbon if the material is deposited in a suitable location; the cores collected in this study suggest that shelf sediment remobilisation has augmented this process. Shallow shelves and slopes are unlikely to serve as long-term sequestration locations, since bioturbation, marine reworking, tectonic uplift and eustatic changes can affect the viability of these regions for long-term carbon storage. However, if infrequent typhoon-generated turbidity currents can harvest material from both the land and the shelf, and deliver this through the canyon to the deep ocean, then the chances of permanently removing the involved CO_2 from the atmosphere and biosphere are greatly improved.

5.3. Morakot organic matter harvesting, dispersal and deposition mechanisms

Organic carbon analysis allows investigation of the harvesting and offshore deposition of multiple terrestrial OC sources in the Gaoping onshore–offshore system. Assuming that the average terrestrial TOC measured in our samples (Endmembers 1 + 2 + 3 for canyon cores = 0.46 wt.%) is representative of the entire Morakot sediment load (285 MT), the storm exported about 1.3 million tonnes of sedimentary OC to the Gaoping Canyon and onwards towards the Manila Trench, which is roughly similar to the export of Coarse Woody Debris by the Gaoping River during Morakot, calculated by West et al. (2011) to be 1.2–2.5 MT. Differences in $\delta^{15}N$ values, and visual observations, suggest that the extreme flooding seen during Morakot conveyed terrestrial biomass and woody debris to the Gaoping Canyon, either directly or via canyon margin slumping during or shortly after the storm, along with large quantities of OC_{petro} from both Plio-Pleistocene sediments in the western foothills of Taiwan and higher-grade metamorphic rocks located in the Central Range, rather than transporting mostly soil carbon as seen during more normal conditions. Efficient reburial of harvested OC_{petro} is important if the organic carbon cycle is to act as a net CO_2 drawdown mechanism (Hilton et al., 2011). Terrestrial biomass appears to have been transported separately from the clastic bedload, since riverbank deposits contain very little $OC_{biosphere}$. Unlike larger turbidite systems, such as the Italian Marnoso-Arenacea Formation (Talling et al., 2012), there is no significant pattern of OC enrichment or fractionation between sand-rich and mud-rich sections of the cored Morakot deposits (see Fig. S1). Within the canyon cores, K1, K12A, K25B, K8, K8X and K15, there is a small increase in TOC in the upper 1–3 cm (usually 0.1–0.2 wt.% C, K8 has a 1 wt.% C increase). This is not correlated with changing grain size distributions — in core K1 there is an increase in proportion sand-sized clasts, in core K12 an increase in mud-sized grains, K8 has a convoluted distribution of TOC and grain sizes throughout the core, and in cores K12 and K8X no grain size distribution changes were observed in the upper few cm. There is also no uniformity of endmember OC component changes — in cores K1, K12A, K25B and K8 the upper core TOC increase is mostly associated with Endmember 1 ($OC_{biosphere} + OC_{petro\text{-}sed}$) whilst in cores K8X and K15 the increased TOC is associated with Endmember 2 ($OC_{petro\text{-}meta}$). We suggest that the short travel distance compared to other turbidite systems may have reduced the amount of density-size sorting within the core such that sandy sections are not OC-poor as reported elsewhere (Talling et al., 2012). Alternatively, organic matter may have been lost preferentially from coarser sediments during diagenesis, with higher hydraulic conductivity permitting circulation of oxygenated fluids.

Sediment transported by Morakot travelled far offshore (Carter et al., 2014). Our core samples likely represent the decelerating tail of the hyperpycnal flow and subsequent hypopycnal delivery, which is verified by Hsu et al. (2014) in the wake of Typhoon Fanapi. They suggest that $OC_{biosphere}$ has been deposited rapidly offshore; core K1 is only 2 km from the river mouth but contains 0.19 wt.% C depth-averaged $OC_{biosphere} + OC_{petro\text{-}sed}$. Radiocarbon analyses from core K1 suggest that OC_{petro} outweighs $OC_{biosphere}$ by three to one in the upper canyon and even more on the canyon sides and shelf, meaning that these extreme events play an important part in the recycling of previously-sequestered organic matter from terrestrial exposure to marine reburial.

Moving down the canyon, samples collected from beside the canyon thalweg show that coarse terrestrial material is generally constrained within the submarine canyon, which has acted as a conduit delivering sediment and organic matter to the deep ocean, with little marine carbon admixture within the canyon itself except in core K8, which may well be an artefact of increased $OC_{biosphere}$ input. The coarse woody debris observed in core K8 supports this theory, and would suggest that $OC_{biosphere}$ can be concentrated into particular depositional/hydrodynamic locations. Canyon side (K11) and shelf (L9) samples are enriched in OC_{marine} and low in $OC_{biosphere}$. Deposition of terrestrial woody debris in submarine sediments requires an increased density, which can be achieved by waterlogging prior to transport in soils and rivers. This may have led to a bimodal distribution of woody debris following Morakot — material harvested from standing biomass would be more likely to disperse along the sea surface, washing up on beaches around Taiwan and as far away as Japan (Doong et al., 2011; Liu et al., 2013), whilst older, waterlogged material could be transported by turbidity currents to the deep ocean.

Shelf cores contained fine sediment, enriched in OC_{marine}, but also rich in terrestrial OC_{petro}. The endmember unmixing calculations showed that core K11A contained 37% OC_{marine}, and the lower sections of core L9 (excluding the core top) contained 27% OC_{marine}. This means that 63–73% of the shelf OC is from a terrestrial source. This uniformly fine material is likely to be delivered by hypopycnal plumes following regular, minor flooding. Samples K11A and L9 have ^{13}C and N/C values more comparable to samples collected in the Gaoping River during regular conditions (Hilton et al., 2010) than to riverbank deposits collected post-Morakot.

In contrast with other well-studied turbidite systems, this study allows a synthesis of results from pre- and post-storm river sediments, identified submarine density flows (Carter et al., 2014) and widely distributed sediment samples suitable for radiocarbon analysis. This is a rare combination; earlier studies are missing at least one of these features. For example, Wheatcroft et al. (1997) studied a single discharge event off the Eel River and found a laterally-dispersed sediment layer rather than sediment density flows; and Amy and Talling (2006) produced an extremely detailed lateral correlation of Miocene turbidites in the Apennines but could not use ^{14}C analysis, constrain the source of the sediment, nor determine the events leading up to the sediment

density flows. The radiocarbon analyses in this study, combined with the endmember-unmixing method, allowed remobilised sedimentary deposits ($OC_{petro\text{-}sed}$) to be separated from freshly-harvested $OC_{biomass}$, demonstrating that it forms a significant part of offshore OC deposits in the Gaoping system. This combination of results and modelling has generated an unusually well constrained case study of significant sediment transport event in a region where natural OC drawdown and sequestration are important parts of the carbon cycle.

6. Conclusion

Typhoon Morakot mobilised a large amount (c.a. 1.3 MT) of organic carbon in Taiwan, in addition to a similar amount of coarse woody debris. The organic carbon was exported through the Gaoping River to the offshore shelf and canyon system. Core samples collected shortly after the storm allowed identification of material most likely deposited during or within days of Typhoon Morakot. Elemental and isotopic analyses allowed sourcing processes and locations to be linked to offshore deposits. In most fossil turbidite systems this connection is lost due to the passage of time. In the Gaoping system, then, sediment harvesting mechanisms during the typhoon were different to those acting during regular fluvial conditions; we calculate that transport of $OC_{biosphere}$ is enhanced relative to $OC_{petro\text{-}meta}$ during extreme events, and that more woody debris and "fresh" OC are delivered relative to soil material. Variations down-canyon suggest that woody debris and $OC_{biosphere}$ can be concentrated into localised deposits. Gaoping Canyon sediments are dominated by terrestrial OC, which is likely to also have been transported further on into the Manila Trench and sequestered along with remobilised OC_{marine}. On the Gaoping shelf OC_{marine} is added to the sediments rather than replacing terrestrial OC through remineralisation and recycling. Measurements and modelling have shown that sediments from these environments are rich in terrestrial organic carbon, and that the Gaoping Canyon has been an efficient conduit for carbon, from both biological and petrological sources, to the deep ocean. Repeated cycles of $OC_{biosphere}$ growth, harvesting and offshore burial, coupled with efficient reburial of OC_{petro}, can lead to a net draw-down of CO_2 from the atmosphere in this setting. Similar work on other systems is needed in order to assess the generality of our observations and their wider implications for global biogeochemical cycles.

Supplementary data to this article can be found online at http://dx.doi.org/10.1016/j.margeo.2015.02.013.

Acknowledgements

RS was supported by an Engineering and Physical Sciences Research Council (EP/P502365/1 and EP/P504120/1) studentship. JTL was supported by grant number NSC 95-2745-M-110-001 for the Fate of Terrestrial–Nonterrestrial Sediments in High Yield Particle–Export River–Sea Systems Program, which provided the cores in this study. We thank Peter Talling for his insightful and constructive comments on the manuscript and a further, anonymous reviewer for generous endorsement.

References

Amy, l., Talling, P., 2006. Anatomy of turbidites and linked debrites based on long distance (120 x 30 km) bed correlation, Marnoso Arenacea Formation, Northern Apennines, Italy. Sedimentology 53, 161–212.

Arndt, S., Jørgensen, B.B., LaRowe, D.E., Middelburg, J.J., Pancost, R.D., Regnier, P., 2013. Quantifying the degradation of organic matter in marine sediments: a review and synthesis. Earth Sci. Rev. 123, 53–86.

Bagnold, R., 1962. Auto-suspension of transported sediment — turbidity currents. Proc. R. Soc. Lond. A Math. Phys. Sci. 265. http://dx.doi.org/10.1098/rspa.1962.0012 (315-&).

Beyssac, O., Goffe, B., Chopin, C., Rouzaud, J., 2002. Raman spectra of carbonaceous material in metasediments: a new geothermometer. J. Metamorph. Geol. 20, 859–871.

Beyssac, O., Simoes, M., Avouac, J., Farley, K., Chen, Yue-Gau, Chan, Yu-Chang, Goffe, B., 2007. Late Cenozoic metamorphic evolution and exhumation of Taiwan. Tectonics 26 (TC6001-1-32).

Carter, L., Gavey, R., Tailing, P.J., Liu, J.T., 2014. Insights into submarine geohazards from breaks in subsea telecommunication cables. Oceanography 27, 58–67.

Chen, W., Ridgway, K., Horng, C., Chen, Y., Shea, K., Yeh, M., 2001. Stratigraphic architecture, magnetostratigraphy, and incised-valley systems of the Pliocene–Pleistocene collisional marine foreland basin of Taiwan. Geol. Soc. Am. Bull. 113, 1249–1271. http://dx.doi.org/10.1130/0016-7606(2001)113<1249:SAMAIV>2.0.CO;2.

Chiang, C.-S., Yu, H.-S., 2008. Evidence of hyperpycnal flows at the head of the meandering Kaoping Canyon off SW Taiwan. Geo-Mar. Lett. 28, 161–169. http://dx.doi.org/10.1007/s00367-007-0098-7.

Chu, H.-J., Pan, T.-Y., Liou, J.-J., 2011. Extreme precipitation estimation with Typhoon Morakot using frequency and spatial analysis. Terr. Atmos. Ocean. Sci. 22, 549–558. http://dx.doi.org/10.3319/TAO.2011.05.10.02(TM) (International Workshop on Typhoon Morakot, Natl Taiwan Univ, Taipei, PEOPLES R CHINA, MAR 25–26, 2010).

Dadson, S., Hovius, N., Chen, H., Dade, W., Hsieh, M., Willett, S., Hu, J., Horng, M., Chen, M., Stark, C., Lague, D., Lin, J., 2003. Links between erosion, runoff variability and seismicity in the Taiwan orogen. Nature 426, 648–651. http://dx.doi.org/10.1038/nature02150.

Dadson, S., Hovius, N., Pegg, S., Dade, W., Horng, M., Chen, H., 2005. Hyperpycnal river flows from an active mountain belt. J. Geophys. Res. Earth Surf. 110, F4. http://dx.doi.org/10.1029/2004JF000244.

Dickens, A., Gelinas, Y., Masiello, C., Wakeham, S., Hedges, J., 2004. Reburial of fossil organic carbon in marine sediments. Nature 427, 336–339. http://dx.doi.org/10.1038/nature02299.

Doong, D.-J., Chuang, H.-C., Shieh, C.-L., Hu, J.-H., 2011. Quantity, distribution, and impacts of coastal driftwood triggered by a typhoon. Mar. Pollut. Bull. 62, 1446–1454. http://dx.doi.org/10.1016/j.marpolbul.2011.04.021.

Galy, V., France-Lanord, C., Beyssac, O., Faure, P., Kudrass, H., Palhol, F., 2007. Efficient organic carbon burial in the Bengal fan sustained by the Himalayan erosional system. Nature 450, 407–410.

Ge, X., Li, T., Zhang, S., Peng, M., 2010. What causes the extremely heavy rainfall in Taiwan during Typhoon Morakot (2009)? Atmos. Sci. Lett. 11, 46–50. http://dx.doi.org/10.1002/asl.255.

Goldsmith, S.T., Carey, A.E., Lyons, W.B., Kao, S.-J., Lee, T.-Y., Chen, J., 2008. Extreme storm events, landscape denudation, and carbon sequestration: typhoon Mindulle, Choshui River, Taiwan. Geology 36, 483–486. http://dx.doi.org/10.1130/G24624A.1.

Hedges, J., Keil, R., 1995. Sedimentary organic-matter preservation — an assessment and speculative synthesis. Mar. Chem. 49, 81–115.

Hilton, R.G., Galy, A., Hovius, N., Chen, M.-C., Horng, M.-J., Chen, H., 2008. Tropical-cyclone-driven erosion of the terrestrial biosphere from mountains. Nat. Geosci. 1, 759–762. http://dx.doi.org/10.1038/ngeo333.

Hilton, R.G., Galy, A., Hovius, N., Horng, M.-J., Chen, H., 2010. The isotopic composition of particulate organic carbon in mountain rivers of Taiwan. Geochim. Cosmochim. Acta 74, 3164–3181. http://dx.doi.org/10.1016/j.gca.2010.03.004.

Hilton, R.G., Galy, A., Hovius, N., Horng, M.-J., Chen, H., 2011. Efficient transport of fossil organic carbon to the ocean by steep mountain rivers: an orogenic carbon sequestration mechanism. Geology 39, 71–74. http://dx.doi.org/10.1130/G31352.1.

Hilton, R.G., Galy, A., Hovius, N., Kao, S.-J., Horng, M.-J., Chen, H., 2012. Climatic and geomorphic controls on the erosion of terrestrial biomass from subtropical mountain forest. Glob. Biogeochem. Cycles 26. http://dx.doi.org/10.1029/2012GB004314.

Hilton, R.G., Galy, A., West, A.J., Hovius, N., Roberts, G.G., 2013. Geomorphic control on the delta N-15 of mountain forests. Biogeosciences 10, 1693–1705. http://dx.doi.org/10.5194/bg-10-1693-2013.

Hsu, R.T., Liu, J.T., Su, C.-C., Kao, S.-J., Chen, S.-N., Kuo, F.-H., Huang, J.C., 2014. On the links between a river's hyperpycnal plume and marine benthic nepheloid layer in the wake of a typhoon. Prog. Oceanogr. 127, 62–73. http://dx.doi.org/10.1016/j.pocean.2014.06.00.

Huh, C.-A., Lin, H.-L., Lin, S., Huang, Y.-W., 2009a. Modern accumulation rates and a budget of sediment off the Gaoping (Kaoping) River, SW Taiwan: a tidal and flood dominated depositional environment around a submarine canyon. J. Mar. Syst. 76, 405–416. http://dx.doi.org/10.1016/j.jmarsys.2007.07.009.

Huh, C.-A., Liu, J.T., Lin, H.-L., Xu, J.P., 2009b. Tidal and flood signatures of settling particles in the Gaoping submarine canyon (SW Taiwan) revealed from radionuclide and flow measurements. Mar. Geol. 267, 8–17. http://dx.doi.org/10.1016/j.margeo.2009.09.001.

Hung, J.-J., Yeh, Y.-T., Huh, C.-A., 2012. Efficient transport of terrestrial particulate carbon in a tectonically-active marginal sea off southwestern Taiwan. Mar. Geol. 315, 29–43. http://dx.doi.org/10.1016/j.margeo.2012.05.006.

Kao, S.J., Lin, F.J., Liu, K.K., 2003. Organic carbon and nitrogen contents and their isotopic compositions in surficial sediments from the East China Sea shelf and the southern Okinawa Trough. Deep-Sea Res. II Top. Stud. Oceanogr. 50, 1203–1217. http://dx.doi.org/10.1016/S0967-0645(03)00018-.

Kao, S.J., Dai, M., Selvaraj, K., Zhai, W., Cai, P., Chen, S.N., Yang, J.Y.T., Liu, J.T., Liu, C.C., Syvitski, J.P.M., 2010. Cyclone-driven deep sea injection of freshwater and heat by hyperpycnal flow in the subtropics. Geophys. Res. Lett. 37, 1–5. http://dx.doi.org/10.1029/2010GL044893.

Kao, S.J., Hilton, R.G., Selvaraj, K., Dai, M., Zehetner, F., Huang, J.C., Hsu, S.C., Sparkes, R., Liu, J.T., Lee, T.Y., Yang, J.Y.T., Galy, A., Xu, X., Hovius, N., 2014. Preservation of terrestrial organic carbon in marine sediments offshore Taiwan: mountain building and atmospheric carbon dioxide sequestration. Earth Surf. Dyn. 2, 127–139.

Kennedy, M.J., Wagner, T., 2011. Clay mineral continental amplifier for marine carbon sequestration in a greenhouse ocean. Proc. Natl. Acad. Sci. U. S. A. 108, 9776–9781. http://dx.doi.org/10.1073/pnas.1018670108.

Liang, W.-D., Tang, T., Yang, Y., Ko, M., Chuang, W.-S., 2003. Upper-ocean currents around Taiwan. Deep-Sea Res. II Top. Stud. Oceanogr. 50, 1085–1105. http://dx.doi.org/10.1016/S0967-0645(03)00011-0.

Liu, J., Kao, S., Huh, C., Hung, C., 2013. Gravity flows associated with flood events and carbon burial: Taiwan as instructional source area. Annu. Rev. Mar. Sci. 5, 47–68.
Liu, J.T., Hung, J.-J., Lin, H.-L., Huh, C.-A., Lee, C.-L., Hsu, R.T., Huang, Y.-W., Chu, J.C., 2009. From suspended particles to strata: the fate of terrestrial substances in the Gaoping (Kaoping) submarine canyon. J. Mar. Syst. 76, 417–432. http://dx.doi.org/10.1016/j.jmarsys.2008.01.010.
Liu, J.T., Wang, Y.-H., Yang, R.J., Hsu, R.T., Kao, S.J., Lin, H.-L., Kuo, F.H., 2012. Cyclone-induced hyperpycnal turbidity currents in a submarine canyon. J. Geophys. Res. 117, C04033. http://dx.doi.org/10.1029/2011JC007630.
Masson, D.G., Huvenne, V.A.I., de Stigter, H.C., Wolff, G.A., Kiriakoulakis, K., Arzola, R.G., Blackbird, S., 2010. Efficient burial of carbon in a submarine canyon. Geology 38, 831–834. http://dx.doi.org/10.1130/G30895.1.
Milliman, J.D., Syvitski, J.P.M., 1992. Geomorphic/tectonic control of sediment discharge to the ocean: the importance of small mountainous rivers. J. Geol. 100, 525–544 (http://www.jstor.org/stable/30068527).
Mulder, T., Cochonat, P., 1996. Classification of offshore mass movements. J. Sediment. Res. 66, 43–57. http://dx.doi.org/10.1306/D42682AC-2B26-11D7-8648000102C1865D.
Mulder, T., Syvitski, J.P., Migeon, S., Faugéres, J.-C., Savoye, B., 2003. Marine hyperpycnal flows: initiation, behavior and related deposits. A review. Mar. Pet. Geol. 20, 861–882. http://dx.doi.org/10.1016/j.marpetgeo.2003.01.003.
Oppo, D., Sun, Y., 2005. Amplitude and timing of sea-surface temperature change in the northern South China Sea: dynamic link to the East Asian monsoon. Geology 33, 785–788. http://dx.doi.org/10.1130/G21867.1.
Ramsey, L.A., Hovius, N., Lague, D., Liu, C.-S., 2006. Topographic characteristics of the submarine Taiwan orogen. J. Geophys. Res. Earth Surf. 111. http://dx.doi.org/10.1029/2005JF000314 n/a–n/a.
Smith, J.C., Galy, A., Hovius, N., Tye, A.M., Turowski, J.M., Schleppi, P., 2013. Runoff-driven export of particulate organic carbon from soil in temperate forested uplands. Earth Planet. Sci. Lett. 365, 198–208. http://dx.doi.org/10.1016/j.epsl.2013.01.027.
Southon, J.R., Santos, G.M., 2007. Life with MC-SNICS. Part II: further ion source development at the Keck carbon cycle AMS facility. Nucl. Inst. Methods Phys. Res. B Beam Interact. Mater. Atoms Appl. Spectrosc. 259, 88–93.
Sparkes, R., Hovius, N., Galy, A., Kumar, R.V., Liu, J.T., 2013. Automated analysis of carbon in powdered geological and environmental samples by Raman spectroscopy. Appl. Spectrosc. 67, 779–788 (http://as.osa.org/abstract.cfm?URI=as-67-7-779).
Stuiver, M., Polach, H.A., 1977. Discussion: reporting 14C data. Radiocarbon 19, 355–363.
Su, C.-C., Tseng, J.-Y., Hsu, H.-H., Chiang, C.-S., Yu, H.-S., Lin, S., Liu, J.T., 2012. Records of submarine natural hazards off SW Taiwan. Geol. Soc. Lond. Spec. Publ. 361, 41–60. http://dx.doi.org/10.1144/SP361.5.
Talling, P.J., Masson, D.G., Sumner, E.J., Malgesini, G., 2012. Subaqueous sediment density flows: depositional processes and deposit types. Sedimentology 59, 1937–2003. http://dx.doi.org/10.1111/j.1365-3091.2012.01353.x.
Teng, L., 1990. Geotectonic evolution of late Cenozoic arc continent collision in Taiwan. Tectonophysics 183, 57–76. http://dx.doi.org/10.1016/0040-1951(90)90188-E (INTERNATIONAL SYMP ON GEODYNAMIC EVOLUTION OF EASTERN EURASIAN MARGIN, PARIS, FRANCE, SEP, 1988).
Weijers, J.W.H., Blaga, C.I., Werne, J.P., Sinninghe Damsté, J., 2009. Microbial membrane lipids in lake sediments as a paleothermometer. PAGES News 17.
Wheatcroft, R., Sommerfield, C., Drake, D., Borgeld, J., Nittrouer, C., 1997. Rapid and widespread dispersal of flood sediment on the northern California margin. Geology 25, 163–166. http://dx.doi.org/10.1130/0091-7613(1997)025<0163:RAWDOF>2.3.CO;2.
West, A.J., Lin, C.W., Lin, T.C., Hilton, R.G., Liu, S.H., Chang, C.T., Lin, K.C., Galy, A., Sparkes, R.B., Hovius, N., 2011. Mobilization and transport of coarse woody debris to the oceans triggered by an extreme tropical storm. Limnol. Oceanogr. 56, 77–85. http://dx.doi.org/10.4319/lo.2011.56.1.0077.
Xu, X., Trumbore, S.E., Zheng, S., Southon, J.R., McDuffee, K.E., Luttgen, M., Liu, J.C., 2007. Modifying a sealed tube zinc reduction method for preparation of AMS graphite targets: reducing background and attaining high precision. Nucl. Inst. Methods Phys. Res. B Beam Interact. Mater. Atoms Appl. Spectrosc. 259, 320–329. http://dx.doi.org/10.1016/j.nimb.2007.01.175 (10th International Conference on Accelerator Mass Spectrometry, Univ Calif Berkeley, Berkeley, CA, SEP 05–10, 2005).